Active feedback cooling of a SiN membrane resonator by electrostatic actuation

Borrielli, A.; Bonaldi, M.; Serra, E.; Sarro, P.M.; Morana, B.

DOI
10.1063/5.0049721

Publication date
2021

Document Version
Final published version

Published in
Journal of Applied Physics

Journal of Applied Physics

Active feedback cooling of a SiN membrane resonator by electrostatic actuation

Cite as: J. Appl. Phys. **130**, 014502 (2021); https://doi.org/10.1063/5.0049721
Submitted: 08 March 2021 . Accepted: 15 June 2021 . Published Online: 06 July 2021

A. Borrielli, M. Bonaldi, E. Serra, P. M. Sarro, and B. Morana

Journal of Applied Physics ARTICLE scitation.org/journal/jap

Active feedback cooling of a SiN membrane resonator by electrostatic actuation

Cite as: J. Appl. Phys. **130**, 014502 (2021); doi: 10.1063/5.0049721
Submitted: 8 March 2021 · Accepted: 15 June 2021 ·
Published Online: 6 July 2021

A. Borrielli,[1,a)] M. Bonaldi,[1] E. Serra,[1,b)] P. M. Sarro,[2] and B. Morana[2]

AFFILIATIONS

[1]Institute of Materials for Electronics and Magnetism, IMEM-CNR, Trento Unit c/o Fondazione Bruno Kessler, Via alla Cascata 56/C, Povo, Trento IT-38123, Italy
[2]Department of Microelectronics and Computer Engineering/ECTM/DIMES, Delft University of Technology, Feldmanweg 17, 2628 CT Delft, Netherlands

[a)]**Author to whom correspondence should be addressed:** borrielli@fbk.eu
[b)]**Also at:** Istituto Nazionale di Fisica Nucleare (INFN), Trento Institute for Fundamental Physics and Application, 38123 Povo, Trento, Italy.

ABSTRACT

Feedback-based control techniques are useful tools in precision measurements as they allow us to actively shape the mechanical response of high quality factor oscillators used in force detection measurements. In this paper, we implement a feedback technique on a high-stress low-loss SiN membrane resonator, exploiting the charges trapped on the dielectric membrane. A properly delayed feedback force (dissipative feedback) enables the narrowing of the thermomechanical displacement variance in a similar manner to the cooling of the normal mechanical mode down to an effective temperature T_{eff}. In the experiment reported here, we started from room temperature and gradually increasing the feedback gain, we were able to cool down the first normal mode of the resonator to a minimum temperature of about 124 mK. This limit is imposed by our experimental setup and, in particular, by the injection of the read-out noise into the feedback. We discuss the implementation details and possible improvements to the technique.

I. INTRODUCTION

Since the pioneering experiments of Coulomb and Cavendish at the end of the 16th century up to the refined Micro/Nano Electro-Mechanical Systems (MEMS/NEMS) devices of today, the simple displacement of a mechanical element has played a key role in sensing a wide variety of very weak phenomena with great accuracy. As a whole, the crucial aspect of these experiments is the ability of converting a weak force to which the mechanical device is subjected into a displacement z or a frequency shift $\Delta\omega$ that are measurable by electrical or optical high-sensitivity transduction methods. The detection of single electron spin,[1] the persistent currents in normal metal rings,[2] and the imprint of quantum phenomena as the force noise associated with the quantized nature of light[3] or the Casimir effect,[4] are just a few of significant achievements that have become possible today.

In recent decades, thanks, in particular, to decisive advances in materials science and in micro-nanofabrication techniques, it has been possible to design and build mechanical force sensors of extraordinary quality, sensitive in the range of the attonewtons (10^{-18} N) at room temperature[5] and zeptonewtons (10^{-21} N) at cryogenic temperatures,[6] under a wide range of technological platforms such as hybrid on-chip structures,[7] carbon nanotubes,[8] and silicon nitride (SiN) trampoline resonators.[9]

In principle, force sensitivity is mainly limited by the thermal driving force experienced by the mechanical device, whose power spectral density (PSD) in thermal equilibrium is set by the fluctuation–dissipation theorem (FDT)[10]

$$S_F = 4k_B T m\omega_0/Q, \tag{1}$$

where k_B is Boltzmann's constant, T is the temperature of the environment, m is the mass, and Q is the mechanical quality factor of the resonator. FDT associates thermal Langevin fluctuating forces with the irreversible losses existing in a resonator, quantified by Q in Eq. (1), making it evident that the fundamental

thermomechanical noise floor, and then the signal-to-noise ratio (SNR) of a mechanical sensor, benefits from a small mass and low mechanical dissipation (high Q). This has justified several decades of research into increasing the quality factor of resonators by reducing the underlying dissipations, leading in recent years into developing devices with unprecedented low mechanical losses.[11,12]

However, in addition to the SNR, the bandwidth of a sensor is important; indeed, increasing the Q also decreases the maximum available bandwidth of the system. High-Q sensors take a long time (inversely proportional to Q) to respond to changes in the external signal because of the long correlation time of the oscillator motion. The seeking of the proper tradeoff between the general requirements of high SNR (low thermomechanical noise floor) and responsiveness to phenomena that quickly vary in time is, therefore, a need in the design and manufacture of a sensor.

A dissipative feedback control of the mechanical system is an effective technique to manage such high quality factors, as those needed to increase the sensitivity, but without placing any restriction on bandwidth. In principle, this can be accomplished if the resonator position is externally monitored through a low noise transduction method, phase shifted, and applied back as force; a conceptual representation of dissipative feedback is illustrated in Fig. 1. This scheme artificially modifies the mechanical transfer function of the resonator in a similar manner to a change in the effective correlation time of the motion (or in the effective quality factor, Q_{eff}), without introducing any alterations to the actual dissipation and then to the thermal fluctuations. These techniques are well established and largely used in a number of fields of physics and engineering; examples can be found in force detection experiments such as those involving ton-scale gravitational wave detectors,[13] atomic force microscopes (AFMs),[14] and optomechanical systems.[7] Since dissipative feedback corresponds to a reduction of the thermomechanical mean-squared displacement (displacement variance), many authors refer to these techniques as *cold damping* or *feedback cooling* defining an effective temperature for the resonant mode as follows:

$$\frac{Q_{eff}}{Q}\frac{k_B T}{m\omega_0^2} = \frac{k_B T_{eff}}{m\omega_0^2}, \tag{2}$$

where $T_{eff} = Q_{eff}\,T/Q$ is the effective temperature of the mode and Q_{eff} is the effective quality factor with Q and T the actual values.

In this paper, we present a feedback technique implemented on a SiN membrane-based electromechanical system and investigate its performances to cool the first mechanical normal mode of the membrane resonator. Starting from room temperature and gradually increasing the feedback gain, we were able to identify a minimum effective temperature T_{eff} of about 124 mK for the coolest normal mode. This limit is mainly due to the injection of the read-out noise into the feedback that restricts the maximum amount of cooling.

This kind of membrane-based resonator has been specifically developed to meet the experimental needs of advanced optomechanical setups. Their optical properties are compatible with their use as optomechanical oscillators,[15] both in Michelson interferometers and in cavity setups.[16] Moreover, their quality factor remains high in the whole frequency range, so they can be used with optimal efficiency, both in single-mode applications, such as optical cooling,[17] and in multimode applications, such as two-mode squeezing.[18] Recently, they have been embedded in a "membrane-in-the-middle" setup, allowing us to reach a thermal occupation number in the transition region from classical to quantum regime[19] and to reveal, through the analysis of motional sidebands asymmetry measured by heterodyne detection,[20] nonclassical properties in the dynamics of macroscopic oscillators.[21]

Here, the feedback was realized by monitoring the thermal motion of the thin membrane (≈100 nm) through a high-sensitivity optical interferometric readout and the feedback force was applied by means of an electrode electrostatically coupled to the trapped charges on the dielectric SiN membrane.

This article is organized as follows: in Sec. II, we discuss the model for the dissipative feedback and its implication on the performances of a force sensor; in Sec. III, we provide some properties of the membrane-based resonators as well as a detailed description of the experimental realization of the feedback cooling, and, finally, in Sec. IV, we discuss the results.

II. DISSIPATIVE FEEDBACK THEORY

In this section, we summarize the standard modeling of the feedback cooling.[22] Figure 1 shows a conceptual diagram of

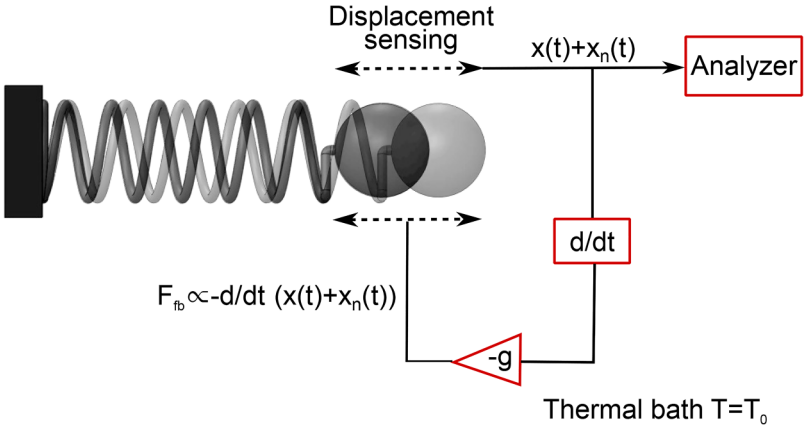

FIG. 1. Conceptual scheme of dissipative feedback applied to a damped harmonic oscillator, here represented by a mass m connected to an elastic element of spring constant k. The oscillator is real-time actuated by a force proportional to the derivative of the thermomechanical displacement signal. With a negative gain, this is equivalent to an additional viscous damping.

dissipative feedback applied to a damped harmonic oscillator, here represented by a mass m, an elastic element of real spring constant k, and an intrinsic dissipation γ_0. The feedback loop consists in monitoring the thermomechanical motion of the oscillator and actuating it by a force proportional to the derivative of the oscillating signal. For a negative gain, this corresponds to an additional viscous damping, similarly to the case of a mechanical oscillator subjected to a force proportional to its velocity. Since in experiments it is more common to analyze the mechanical motion in the frequency domain as a noise spectrum, we will examine the effect of such a feedback force on the spectral features of the thermomechanical motion.

A harmonic oscillator under the condition depicted in Fig. 1 can be described by the Langevin equations written in the frequency domain as

$$\begin{aligned} i\omega x(\omega) &= v(\omega), \\ i\omega x_n(\omega) &= v_n(\omega), \\ i\omega v(\omega) &= -\frac{\gamma_0}{m}v(\omega) - \omega_0^2 x(\omega) + \frac{1}{m}\xi_{th}(\omega) - \frac{g\gamma_0}{m}(v(\omega) + v_n(\omega)), \end{aligned} \tag{3}$$

where $\omega_0 = \sqrt{k/m}$ is the angular resonance frequency, g is an electronic gain, x_n is the read-out noise, and $\xi_{th}(\omega)$ is the frequency component of the random thermal Langevin force with spectral density given by Eq. (1). The last term of Eq. (3) represents the additional viscous force provided by the feedback, and for a more complete modeling of the system, it also includes the contribution of the measurement noise on the displacement signal, considering that the measured displacement is $x + x_n$. We can solve Eq. (3) for $x(\omega)$ in terms of the fluctuating force and the measurements noise to obtain

$$x(\omega) = \frac{\frac{1}{m}(\xi_{th}(\omega) - ig\gamma_0\omega x_n(\omega))}{(\omega_0^2 - \omega^2) + \frac{1}{m}i(1+g)\gamma_0\omega}, \tag{4}$$

with power spectral density

$$S_x(\omega) = \frac{1/m^2}{(\omega_0^2 - \omega^2)^2 + (1+g)^2\omega_0^2\omega^2/Q^2}S_F + \frac{g^2\omega_0^2\omega^2/Q^2}{(\omega_0^2 - \omega^2)^2 + (1+g)^2\omega_0^2\omega^2/Q^2}S_{x_n}, \tag{5}$$

where S_F is the spectral density of the thermal noise force, which depends on the resonator dissipation according to the fluctuation–dissipation theorem [Eq. (1)] and S_{x_n} is the spectral density of the measurement noise. Considering that our experimental setup allows a measure of the mechanical dissipation through the quality factor Q (cf. Sec. III), in writing Eq. (5), we express the dissipation γ_0 in terms of the oscillator's intrinsic quality factor[23] according to $\gamma_0 = m\omega_0/Q$. Now, we are able to fix some general features of the feedback scheme presented in Fig. 1 and in Sec. III, we will describe a practical implementation of it.

A. Cold damping

Figure 2 shows the normalized thermomechanical displacement power spectral density [Eq. (5)] for $g = 0$ (i.e., without feedback) and for increased feedback gains. The dissipative feedback loop does not change the thermal noise floor that is ultimately set by the intrinsic dissipation of the resonator at the bath temperature. At frequency sufficiently below the resonance ($\omega \ll \omega_0$), the spectral density is approximately flat with noise floor $\approx \sqrt{4k_BT/k\omega_0 Q}$. The increase of the feedback gain only modifies the thermal displacement noise at frequencies close to resonance, and as the most noise power is concentrated there, one can observe a gradual decreasing of the integrated area under the thermomechanical displacement power spectral density (PSD). According to the equipartition theorem, we can define the mode temperature of the oscillator as $T_{eff} = k\sigma_x^2/k_B$, where σ_x^2 represents the variance of the mechanical displacement that is related to the integrated area of the PSD by the relation

$$\sigma_x^2 = \frac{1}{2\pi}\int_0^\infty S_x(\omega)d\omega. \tag{6}$$

The consequence of the dissipative feedback is thus a progressive reduction of the effective mode temperature (or equivalently the variance of the thermomechanical noise), which depends on the

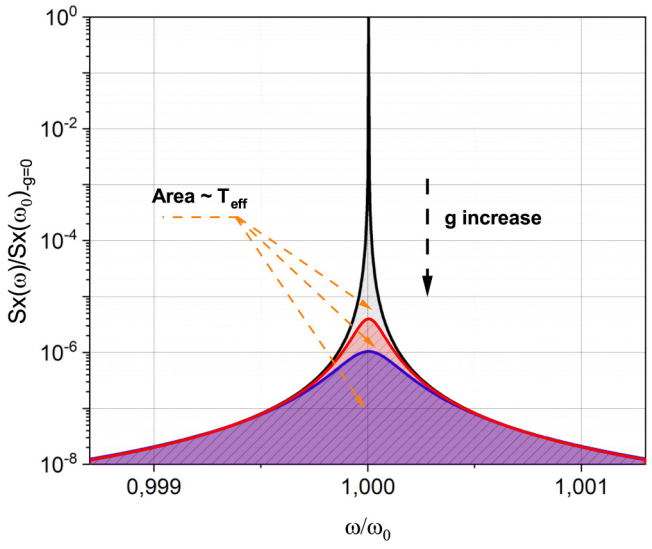

FIG. 2. Normalized thermomechanical displacement power spectral density (PSD) in a damped resonator under the effect of a dissipative feedback. Increasing the feedback gain only changes the thermal noise around the resonance, thus observing a gradual decrease of the integrated area that corresponds to a reduction of the effective resonator temperature. PSD was calculated for a resonator with $Q = 3.5$ M (condition equivalent to the SiN membrane resonators described in the experimental section) under low gain regime; therefore, only the first term of (5) was used.

feedback gain. Using (5) and (6), we find

$$T_{eff} = \frac{T_0}{1+g} + \left(\frac{g^2}{1+g}\right)\frac{k\omega_0}{4k_B Q} S_{x_n}, \tag{7}$$

where T_0 is the thermal bath temperature. The second term of (7) is due to the injection of the measurement noise (uncorrelated to the Langevin force) into the feedback signal, which imposes a competing heating growing with the feedback gain. The upshot is, therefore, a minimum achievable temperature of

$$T_{min} = 2T_0 \frac{\sqrt{1+SNR}-1}{SNR} \tag{8}$$

at $g = \sqrt{1+SNR}-1$, where $SNR = 4k_B Q T_0/k\omega_0 S_{x_n}$ is the ratio between thermomechanical noise and readout noise at resonance without feedback. In the limit of low gain regime ($g \ll \sqrt{1+SNR}-1$), the effect of the measurement noise can be neglected because the first term of (7) is order of magnitudes higher than the second term and T_{eff} reduces to the familiar form[24] $T_0/(1+g)$; on the other hand, at high gains ($g > \sqrt{1+SNR}-1$), the transduction noise sent back to the actuator causes net heating of the vibrational mode. Nevertheless, we stress that the mode temperature T_{eff} is not a comprehensive property of the system; rather, it depicts a single mode of resonance that is pumped out the thermal equilibrium. The bulk temperature in negligibly affected with single-mode temperature tuning, because most of the degrees of freedom in the system are not modified by feedback.[25,26]

B. Noise squashing

A critical aspect of the feedback scheme shown in Fig. 1 can be observed at strong gain, when the motion of the mechanical device is driven by the transduction noise rather than the thermal Langevin force, and, consequently, it becomes correlated to the noise on the detector. In an in-loop transduction scheme, the power spectral density of the measured displacement $x + x_n$ can be written as

$$S_{x+x_n}(\omega) = \frac{1/m^2}{(\omega_0^2-\omega^2)^2 + (1+g)^2\omega_0^2\omega^2/Q^2} S_F + \frac{(\omega_0^2-\omega^2)^2 + \omega_0^2\omega^2/Q^2}{(\omega_0^2-\omega^2)^2 + (1+g)^2\omega_0^2\omega^2/Q^2} S_{x_n}. \tag{9}$$

The difference between Eq. (5) and Eq. (9) is schematized in Fig. 3, where we calculated the power spectral densities at resonance vs the feedback gain using the parameters listed in Table I, which refer to the SiN membrane resonator and the experimental setup detailed in Sec. III. As mentioned earlier, the effect of the dissipative feedback is a progressive drop of the displacement PSD at resonance and hence the cooling of the mechanical mode. Sufficiently far from the critical gain ($g \ll \sqrt{1+SNR}-1 \approx 4600$), the displacement remains thermal-driven an then uncorrelated from the transduction noise. In this case, S_{x+x_n} reduces to S_x and the mode temperature is proportional to the integrated area between the measured transduction spectra an the transduction noise.[22] On the other hand, at higher g, the actual displacement power noise tends to the noise floor S_{x_n} but the measured

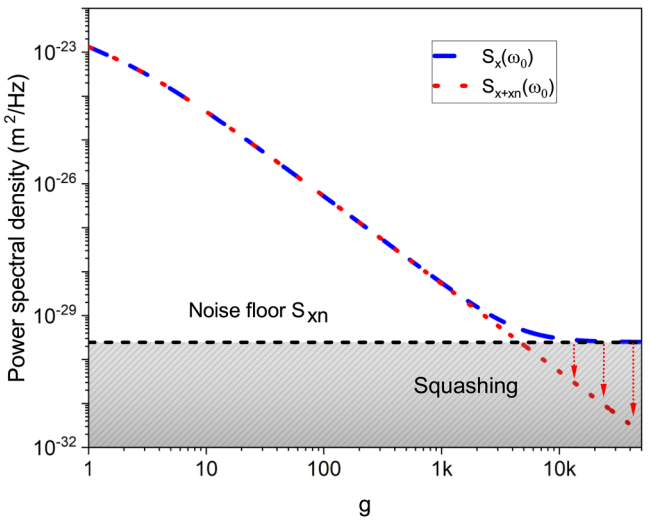

FIG. 3. Comparison between the power spectral densities corresponding to the actual displacement (5) and the measured one (9). Spectra were calculated at the resonance frequency using the real parameters of the experiment listed in Table I. For large gains, the feedback leads to correlations between the resonator displacement and the detector noise, thus changing the shape of the measured power spectrum that is squashed below the detector noise around the resonance.

one is reduced below it. This "squashing" of the noise spectra below the noise of the detector is due to feedback-induced anticorrelations between the detector noise and the noise-driven displacement and produces unphysical results if the mechanical mode temperature is inferred from the measured power spectra, by simply subtracting the noise floor. Lee *et al.*[27] showed as an independent out-of-loop transduction permits of inferring a mode temperature in good agreement with the prediction of Eq. (7), even above the critical gain.

C. Force sensing resolution

Linear feedback cooling is a common procedure to increase the bandwidth and reduce the variance of thermal fluctuations in a resonant device. For example, atomic force microscopes (AFMs) use a tip hosted in resonant cantilevers as force sensor to map the topography of a surface at the atomic scale, ultimately by sensing the atomic force between the tip and the surface. That resolution

TABLE I. Parameters characterizing the fundamental mode (0, 1) considered for the feedback, as well as other relevant parameters concerning both the membrane and the measuring system. The modal mass m is extracted as fit parameter from Fig. 5(a) with an error of $\pm 10\%$. The other quantities are obtained from independent measurements with an error below 2%.

m (μg)	ρ (g/cm^3)	σ (GPa)	f (kHz)	R (mm)	Q	S_{x_n} (m^2/Hz)
0.21	2.8	0.83	269	0.77	3.5×10^6	2.3×10^{-30}

requires very low thermal noise floor, and therefore high-Q resonators. Under these conditions, the corresponding bandwidth ($\propto 1/Q$) results in a very long response time and, therefore, an excessive time to scan the surface to be analyzed. Dissipative feedback instead allows us to improve the bandwidth and, therefore, the imaging speed without degrading the SNR.[14] Moreover, linear feedback is commonly used to stabilize the tip-surface separation in non-contact configuration AFM, thus avoiding collisions and suppressing frequency drifts.[28]

A more advanced task of oscillator-based force sensors is in detecting a weak signal force F_{sig} with (flat) spectral density well below the thermal background force ($S_F^{sig} \ll S_F^{th}$), i.e., when the input force is buried on the thermal noise. In Ref. 7, Gavartin *et al.* experimentally demonstrated the powerful role of a dissipative feedback protocol in resolving this force against the thermal noise. Indeed, as long as the energy averaging is chosen as estimator of the force magnitude, the force resolution scales as $\sqrt[4]{\tau_c/\tau}$, where τ is the averaging time and τ_c is the correlation time of the oscillator. Thus, cold damping represents a way to effectively improve the convergence of the energy averaging by reducing the correlation time. In that regard, however, we must to point out that:

- stationary linear feedback does not improve the accuracy with which the oscillator position can be determined (i.e., the signal-to-noise ratio), this is because the feedback modifies the transfer function of the resonator and then its response to input excitations, regardless of whether the input is a signal or a background force;
- as discussed elsewhere,[29,30] the force estimation process founded on feedback-assisted reduction of the effective resonator time constant is not necessarily optimal. Indeed, the position measurement recorded with and without feedback is linked by a completely deterministic relation; therefore, a proper filtering of the position record without feedback can completely replace the feedback even in the case of nonstationary, non-Gaussian input; and
- appropriate post-processing data filtering requires accurate knowledge of the susceptibility of the mechanical system that is nontrivial especially for micro-optomechanical systems, where the stability of the resonance is affected by several detrimental effects. Stabilization of oscillator parameters and dynamics is thus a crucial issue.[31,32]

III. EXPERIMENTAL REALIZATION OF THE FEEDBACK COOLING

A. Silicon-nitride resonators

The mechanical resonator used throughout the paper for the implementation of the feedback-cooling is a circularly shaped tensioned SiN membrane, specifically developed to be embedded in advanced optomechanical setups. Nano-strings or membranes obtained from SiN films have attracted considerable attention due to the possibility of exploiting the "dilution" of the intrinsic dissipation, usually high in amorphous materials, leading to flexural mechanical modes with very high quality factors. This effect, first considered in the design of mirror's suspensions in gravitational wave antennae,[33] occurs when the SiN layer is produced with residual stress, which is tensile and high enough to push the device to a regime, where the mechanical behavior is governed by the internal stress of the layer and the flexural rigidity can be neglected.[34] Dissipation dilution effects can be observed in very thin strings or membranes with thicknesses smaller than 100 nm and residual stress starting from about 1 GPa. The use of these structures combined with efficient solutions to isolate them from their support has allowed realizing resonators with exceptionally high Q factors.[11,12]

In the field of optomechanics, systems based on a SiN membrane oscillator have shown for the first time the mechanical effect of the quantum noise in the light[3] and one of the first observations of pondero-motive light squeezing.[35] In many cases, the oscillators consist of commercially available free-standing SiN membranes having residual tensile stress of 1 GPa. However, in this case, the mechanical quality factors of many millions in principle obtainable, thanks to the high tensile stress, cannot be achieved due to the mechanical losses. These are strongly dependent on the mounting, especially for the low frequency modes, and are the cause of scattered Q-factors based on the modal form.[36]

Recently, we proposed a way to overcome the limitations of commercial membranes by addressing the issue of mechanical losses employing a coupled oscillators model,[37] where the vibrations of the membrane are considered along with those of the silicon chip. This approach resulted in the design and realization of a "loss shield" structure on which the membrane is embedded [Fig. 4(a)]. In these devices, almost all of the vibrations of the membrane have a high quality factor and reach the limit set by the intrinsic dissipation. The production of these devices has required the development of a specific manufacturing process[38] based on MEMS bulk micro-machining by Deep-Reaction Ion Etching (DRIE) and through two-side wafer processing.

The SiN employed for the realization of the circularly shaped membranes was obtained by means of LPCVD (Low-Pressure Chemical Vapor Deposition) using DCS (dichlorosilane) and NH_3 (ammonia) as gas precursors. The gas flows were tuned to obtain a SiN layer with a composition close to stoichiometry (Si_3N_4) and a resulting residual tensile stress close to 1 GPa. The deposition time was tuned to obtain a SiN layer with a thickness of 100 nm. Although a layer with higher stress and lower thickness would have allowed to improve the mechanical performance, owing to a greater dilution effect and less dissipation, the above values were selected as they offered a good tradeoff. More specifically, such layers allowed high mechanical quality factors (Q), low absorption of the film at the laser wavelength used in our optomechanical setups (1064 nm), and the required robustness for the achievement of large-area membranes capable of withstanding all the necessary fabrication and subsequent cleaning and handling steps. The residual tensile stress, measured by the wafer curvature method and confirmed by the resonance frequencies of the device, was slightly lower (0.83 GPa) than the target value of 1 GPa. Most likely, this was due to not perfect control of the deposition pressure of the employed LPCVD system. The film thickness and the refractive index were determined by variable-angle spectroscopic ellipsometry. The thickness resulted in compliance with the nominal value within 5%. The refractive index of the film at 1064 nm was instead $n = 1.993$ with the error below 1%, this is slightly different from that of a perfectly stoichiometric SiN film, which is $n = 2$ at

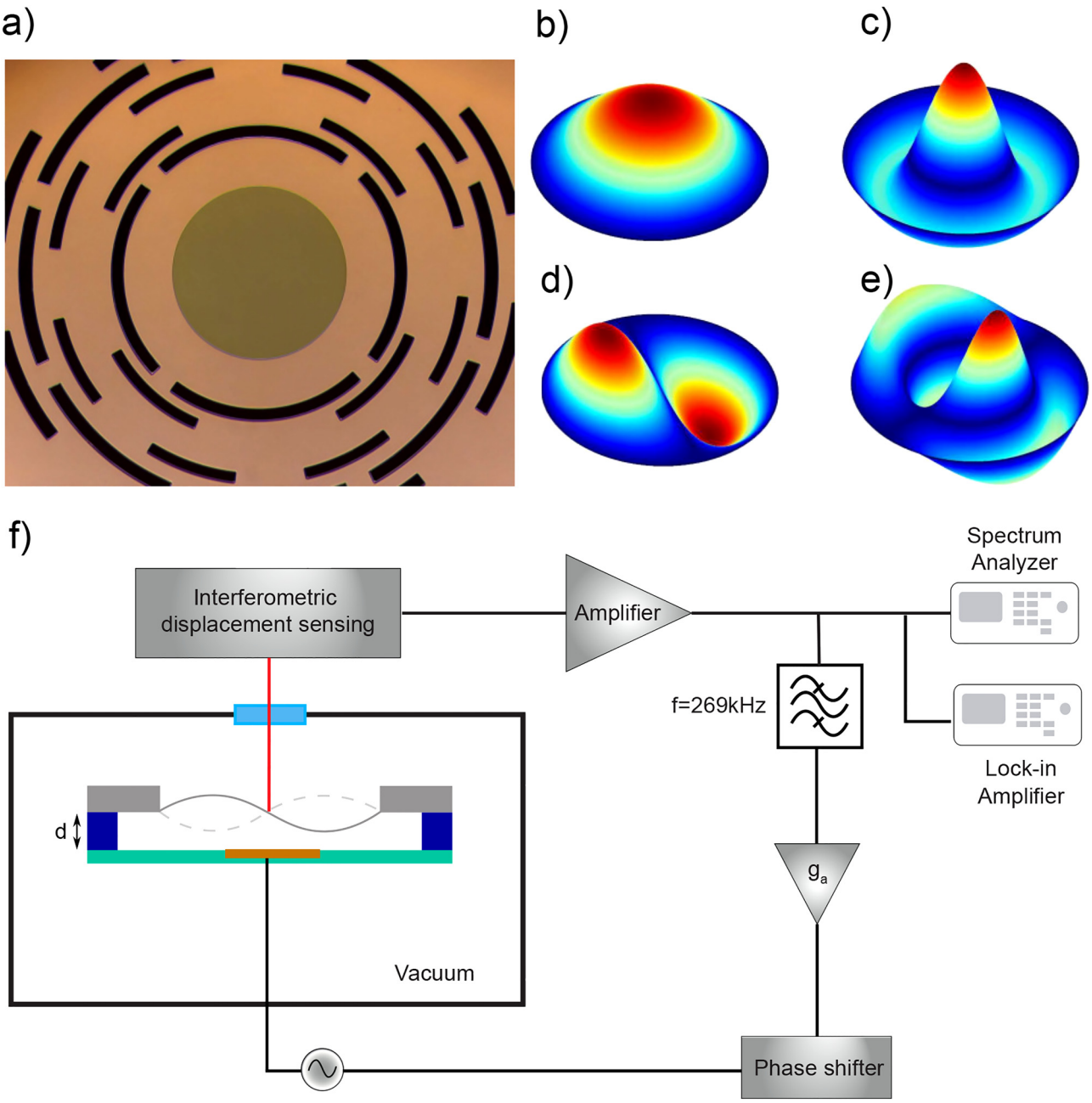

FIG. 4. (a) Optical microscope picture of the circular membrane, with diameter 1.55 mm and thickness 100 nm. The membrane is mechanically supported by silicon structure acting as "loss shield."[37] (b)–(e) Modal shapes of the first four membrane modes, resonating at frequencies between 269 and 621 kHz. (f) Scheme of the feedback loop realized by an interferometric displacement sensing and an electrostatic actuation of the membrane.

1064 nm. This was expected as the gas flow ratio (DCS/NH_3) specifically set to obtain residual tensile stress at the target value was slightly lower compared to the one used for the deposition of Si_3N_4 in the employed LPCVD system.

B. Experimental setup

The experimental setup used for the implementation of the feedback cooling is shown in Fig. 4(f) and includes a displacement

sensing section and a feedback-controlled actuation section. The first one is described in detail elsewhere[38] and basically consists of a polarization-sensitive Michelson interferometer with displacement sensitivity of about 10^{-30} m^2/Hz. Here, it is employed to sense the thermomechanical noise of the tensioned membranes. Circular tensioned membranes have normal modes whose frequencies are given by the expression $f_{mn} = \frac{1}{2\pi}\sqrt{\frac{\sigma}{\rho}}\frac{1}{R}\alpha_{mn}$, where σ is the stress, ρ the density, R the radius of the membrane, and α_{mn} is the nth root of the first kind Bessel function of order m. Figures 4(b)–4(e) show the modal shapes of the first four modes [with indexes (0,1) (0,2) (1,1), and (1,2)]. In the present work, the feedback cooling was realized on the first mode (0,1) with frequency about 269 kHz.

The feedback force was applied by an electrostatic actuation scheme as depicted in Fig. 4(f). A circular electrode realized on a printed circuit board (PCB) is firmly clamped to the silicon chip supporting the membrane and it is held at distance $d \approx 300\,\mu$m from it by calibrated spacers. The actuation of the membrane is controlled by the voltage V applied to the electrode through an external circuit. In such a configuration, several phenomena could contribute to impart forces on the membrane, which can be either electrostatic, due to the fixed charges ordinarily accumulated on the surface of dielectric medium as SiN, or dielectric in case a static voltage V_{dc} polarizes the dielectric device, which, in turn, is subjected to an attractive force. In both cases, the forces can be modulated at high frequency and several groups reported effective methodologies of electrostatic transduction/activation, integrated on MEMS/NEMS devices.[39–41]

We characterized the forces, imparted on the resonator by the actuation system of Fig. 4(f), by applying both a bias voltage V_{dc} and a weak modulation voltage V_{ac} to the electrode and sending the displacement signal to a lock-in amplifier (HF2LI Zurich Instruments). With this scheme, we drove the mechanical resonance of the membrane performing three different sets of tests. First, we have varied V_{dc} in the range 0–10 V and kept V_{ac} at a fixed value of 5 mV with a modulation frequency equal to the mechanical resonance frequency of the first normal mode of the membrane ($f_0 = 269$ kHz). The amplitude of the mechanical oscillation recorded by the lock-in was found to be independent from the value of V_{dc}, which excludes effects of dielectric forces that would instead be dependent on the applied bias voltage. Second, we set V_{dc} at zero and varied V_{ac} in the range 1–10 mV at the resonance frequency. In this case, the mechanical response of the membrane was linear with V_{ac}. Finally, in order to verify the presence or absence of force components proportional to V_{ac}^2, we applied a variable voltage V_{ac} at half the mechanical resonance frequency $f_0/2$, noting the absence of any effect on the resonant mode. These three tests allow us to conclude that in this case, the membrane actuation is linear and it occurs by purely electrostatic effects due to the accumulation of trapped charges on the dielectric membrane. The charging of SiN layers is a well-known phenomenon due to the capture of charges by trapping centers originating from a specific structural defect in amorphous silicon nitride.[42]

Another relevant point to check for the feedback experiment is the stability of the electric charge. In fact, the overall feedback gain g is set by a combination of an adjustable gain amplifier g_a and of a transduction gain g_t, so that $g = g_a g_t$, where g_t depends on the electric charge. We have verified that the electric charge remains constant over time (at least in the period of observation, which was 1 day) if the experimental setup remains under vacuum; therefore, g_t can be considered a constant parameter in the feedback experiment, and as discussed in Sec. III C, it is derived as fit parameter.

The feedback loop consists of an amplifier, a bandpass filter, and a phase shifter [Fig. 4(f)]. The need for the filters is determined by the presence of a variety of membrane oscillation modes, with frequencies and modal shapes different from the fundamental mode considered in this work. To realize a dissipative feedback and avoid self-oscillation of the mechanical system, the feedback force should be proportional and opposite to the speed of the displacement, therefore having a time lag corresponding to $-90°$, at all frequencies corresponding to the modal forms. This is very difficult for two reasons:

1. the phase shift in an analog circuit is usually introduced with a combination of bandpass filters; therefore, being frequency-dependent, it cannot keep a constant value over a wideband; and
2. higher order modes have radial and/or circumferential nodal lines, so the overall displacement of the membrane is the overlapping of modal shapes that can move in opposite directions, even if at different frequencies. Therefore, moving from one mode to another may require not only an adjustment of the phase but also a change of sign of implementation. The problem is practically insurmountable in the case of mechanical doubles, which move with opposite phases and can have only a few tens of Hz difference.

Since a force applied with the wrong phase can activate self-oscillations of the system, electromechanical feedback is only possible on normal modes with enough separate frequencies so that the bandpass filter makes negligible the force applied to the mechanical modes nearby in frequency. In addition to the fundamental mode, in a round membrane, the possible candidates are all modes with axial symmetry and therefore without radial nodal lines. Moreover, since the modal density increases strongly with frequency, the possible candidates are to be searched among the modes with lower frequency. To allow the use of a high feedback gain in the cooling experiment, we implemented a cascade of multi-polar LC filters to a total order of 7. To reduce the cross talk between input and output of the filter system, the filter cascade was built into two shielded boxes, separated by a variable gain amplifier g_a with an adjustable phase shifter.

Finally, the whole experimental setup is accommodated in a vibration isolated vacuum chamber, at a base pressure of 10^{-6} mbar, to suppress gas damping effects on the resonator properties.

C. Experimental observation of cold damping

As a first step, we have characterized the resonant mode of the membrane in terms of resonance frequency and mechanical quality factor at room temperature and without feedback. The quality factor was evaluated by the ring-down method, i.e., the resonator was first forced at the resonance frequency by means of a piezoelectric crystal fixed to the sample holder, and then the drive voltage was removed and the vibration recorded during the decay. The decay time of the

mode gives a direct estimation of the Q-factor.[38] The measured Q was 3.5×10^6, appreciably lower than the typical value[37] for this type of membrane ($\approx 10^7$), probably due to some contamination of the membrane surfaces during electrode clamping.

Second, we used a spectrum analyzer to measure the displacement spectral density of the membrane around the resonance mode of interest with the system disconnected from the feedback ($g = 0$) [Fig. 5(a)]. This first spectrum allowed us to calibrate the effective modal mass by fitting the spectral density data to Eq. (9), where all other parameters have been measured independently. Note that for $g = 0$ Eq. (9) reduces to the more familiar form given in.[10] Modal mass was found to be of 0.21 ± 0.02 μg, in agreement with the theoretical values.[16] In Table I, we summarize the parameters characterizing the fundamental mode (0, 1) considered for the feedback, as well as other relevant parameters concerning both the membrane and the measuring system.

Finally, we turned on the feedback and we progressively increased the feedback gain by tuning the amplifier gain g_a. In Figs. 5(b)–5(d), we show a set of displacement spectral densities obtained for three different values of g_a. The effective mode temperatures shown in Fig. 5 are inferred by fitting the experimental spectra to Eq. (9) and by substituting the extracted parameters to Eq. (7) . The fits comprise three free parameters ω_0, S_{x_n}, and the overall feedback gain g, that in the three examples shown is 36, 865, and 3627, respectively, with an error of $\pm 10\%$. As discussed in Sec. II, the feedback force applied with the right phase results in a cooling of the mechanical mode and the effective modal temperature drops from room temperature at $g = 0$ down to $T_{eff} = 124 \pm 12$ mK at $g = 3627$, which is the minimum temperature reached in this experiment.

Note that if the gain remains well below the critical value defined in Sec. II A, which in this specific case is ≈4600, the observed thermal noise spectra are orders of magnitude higher

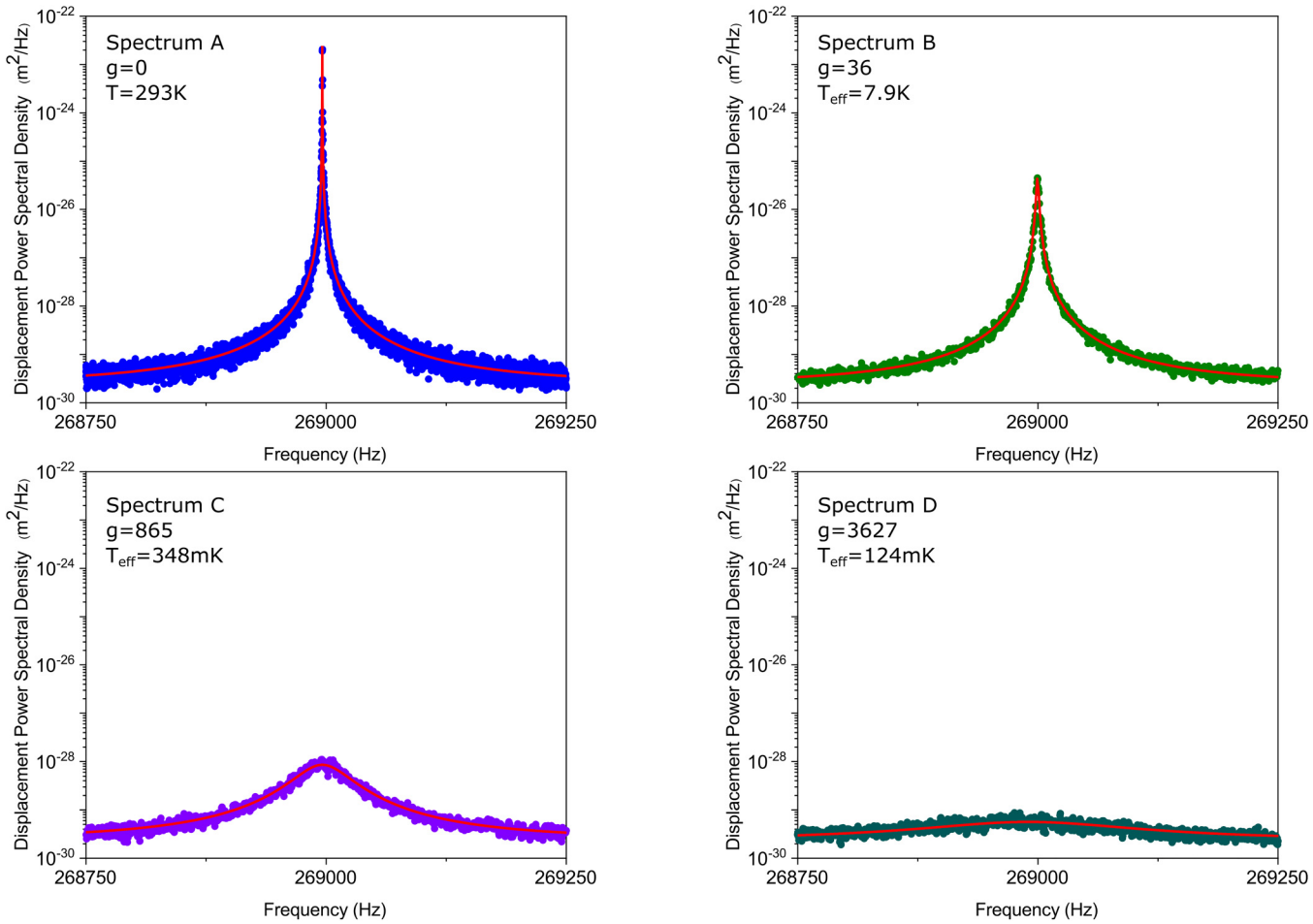

FIG. 5. Cold damping observed on the measured spectral densities of the first resonant mode. Spectrum A represents the oscillator in thermal equilibrium ($g = 0$) at room temperature (293 K) while B–D are obtained for different feedback gains. The effective mode temperatures reported in spectra B–D are inferred by fitting the experimental spectra to Eq. (9) (red lines) and by substituting the extracted parameters to Eq. (7). The inferred gains and mode temperatures are given with an error of $\pm 10\%$.

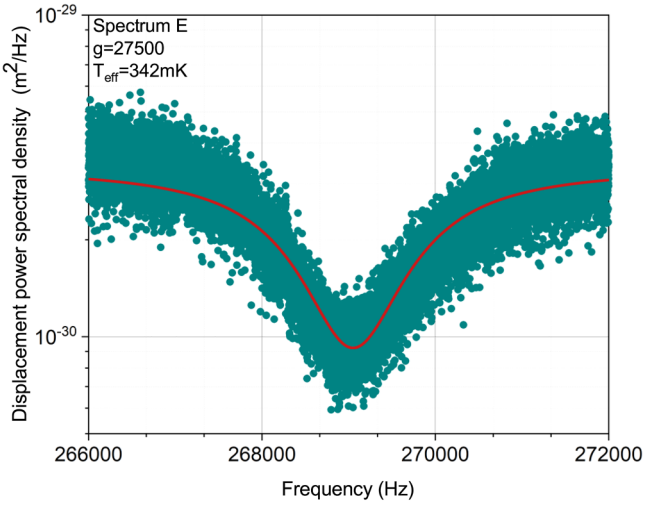

FIG. 6. Distortion of the displacement noise caused by feedback-induced correlations with the detector noise at high gain regime. At this gain level, the feedback heats the resonator rather than cool it, and the effective temperature is inferred by fitting the data to (9) and using (7) . Alternatively, a second detector (out of loop) could be used to measure the resonator motion.[27]

than the measurement noise, which implies that the mode temperature could be well determined also by the area between the observed spectra and the noise floor. Such a condition occurs for spectra A–C of Fig. 5, but it is no longer valid for spectrum D where the gain is close to the critical one and only Eq. (7) allows an accurate temperature estimation.

A further increase of the gain causes a fall of the observed thermal noise below to the white noise floor marking the noise limit of the transduction system, and this "squashing" is shown in Fig. 6 for $g = 27\,500$. As discussed in Sec. II B, at this gain level, the feedback loop has the opposite effect to the desired, exciting the resonator rather than damping it; as a result, an increase of the mode temperature is observed.

A suggestive evolution of this cold-damping scheme could be to replicate n times the pair bandpass filter/phase shifter of Fig. 4(f) so as to cool all the resonant modes with frequencies $f_1 \cdots f_n$ included in a wide range. This multimode cold damping could lead to the partial refrigeration of the mechanical resonator, in contrast to the single-mode cooling that leaves the overall temperature of the object largely unaltered. Recently, the possibility of efficiently extracting thermal energy from many vibrational modes via cold-damping feedback has been predicted under the condition of frequency-resolved resonators.[43] This condition, however, is virtually inapplicable to the membrane resonator used throughout the article, mostly due to the mechanical doublets occurring for non-axisymmetric mechanical modes (with index $m \neq 0$) that are separated by few tens of Hz (cf. Sec. III B).

IV. DISCUSSION AND CONCLUSIONS

In this work, we have detailed the realization of a strong feedback cooling on the first normal mode of a tensioned SiN membrane. We exploited a viscous feedback electrostatic force that increases the damping of the resonator without adding thermal fluctuations. Starting from room temperature, we were able to measure a 3 orders of magnitude reduction of the effective modal temperature, reaching the limits imposed by the read-out. The scheme here adopted takes advantage of the trapped charges on the large-area dielectric SiN membrane and represents an easy system of manipulation and displacement control for that kind of devices. It is simple to achieve by not requiring high DC voltage to actuate the device, with noticeable benefits in terms of reduction in the complexity of the experimental setup, and the actuation electrodes could be easily built-in on the device chip at the microfabrication stage. Also, it is, in principle, compatible with more complex optomechanical setups as, for example, the cavity detuning control in a membrane-in-the-middle optomechanical configuration.[44]

In that regard, it is worth pointing out that micromechanical resonators as SiN membranes coupled to optical technologies represent a promising platform to test quantum limits of resonant sensors or more in general quantum non-classical behavior in macroscopic objects.[20,21] An important prerequisite for approaching the quantum realm in a resonant device is that it is into its quantum ground state. At any non-zero temperature, there is always a finite probability to find the resonator in an excited state, and the average thermal occupation is[45] $\langle n \rangle \approx k_B T/\hbar\omega_0 - 1/2$. When $\langle n \rangle = 1$, the probability finding the resonator in the ground state is 50%, and this means that $\langle n \rangle \leq 1$ indicates that the resonator is into its ground state most of the time. This is achievable with ultra-high frequency resonators ($f \geq$ GHz) in a dilution refrigerator ($T \approx 50$ mK), but lower-frequency resonators and higher

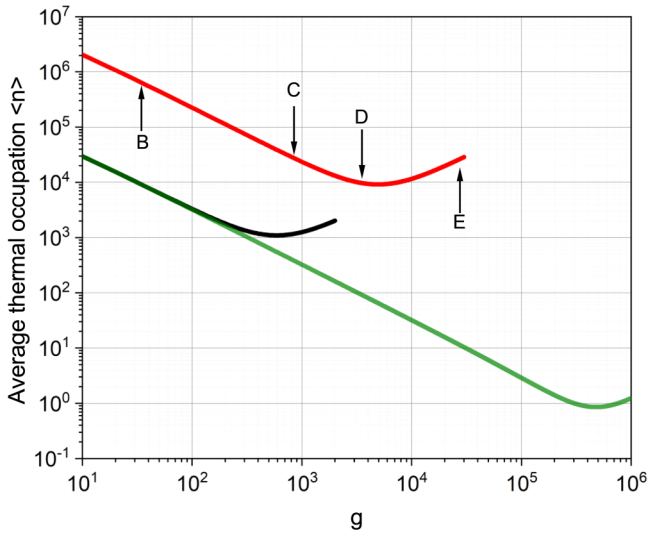

FIG. 7. Evaluation of the average thermal occupation obtainable by active feedback cooling. An upgrade to liquid helium temperature of the experimental setup would allow us to improve the results reported in the paper (red line) up to $\langle n \rangle \approx 1000$ (black line). Cooling the membrane to its ground state ($\langle n \rangle \leq 1$) would require a measurement noise reduced to 10^{-35} m^2/Hz.

environment temperature require cooling techniques as the active feedback cooling here reported or sideband cooling.[46]

Although in our experiment at room temperature, we have reached a modest average occupation number $\langle n \rangle \approx 10^4$, this figure could be greatly reduced by improving the parameters limiting the maximum available amount of cooling, i.e., the thermal bath temperature T_0, the quality factor of the resonant mode, and especially the read-out noise injected into the feedback. As an example in Fig. 7, we compare the results obtained in the experiment presented in the paper with those expected in a state-of-the-art experimental setup. The red line shows the trend of the average thermal occupation number as a function of the feedback gain, calculated on the basis of (7) and by using the experimental parameters of Table I. In the curve, we marked the positions corresponding to the spectra B, C, D, and E reported in Figs. 5 and 6. The black line is instead an evaluation of the thermal occupation number expected if the same experiment would be conducted at 4.2 K, the base temperature of standard cryogenic systems based on liquid helium. Finally, with the green curve, we show how it is possible to obtain a near ground state final occupation number ≈0.8 for a resonator with a quality factor of 10 M, that is, the standard for the SiN membrane considered here by reducing the measurement noise up to 10^{-35} m^2/Hz which can be attained in readout configurations based on optomechanical cavities.[35]

ACKNOWLEDGMENTS

This research was performed within the Project QuaSeRT funded by the QuantERA ERA-NET Cofund in Quantum Technologies implemented within the European Union's Horizon 2020 Programme. This research has been partially supported by INFN (HUMOR Project).

DATA AVAILABILITY

The data that support the findings of this study are available from the corresponding author upon reasonable request.

REFERENCES

[1]D. Rugar, R. Budakian, H. Mamin, and B. Chui, Nature **430**, 329 (2004).
[2]M. Castellanos-Beltran, D. Ngo, W. Shanks, A. Jayich, and J. Harris, Phys. Rev. Lett. **110**, 156801 (2013).
[3]T. Purdy, R. Peterson, and C. Regal, Science **339**, 801 (2013).
[4]M. Bordag, U. Mohideen, and V. Mostepanenko, Phys. Rep. **353**, 1 (2001).
[5]K. Yasumura, T. Stowe, E. Chow, T. Pfafman, T. Kenny, B. Stipe, and D. Rugar, J. Microelectromech. Syst. **9**, 117 (2000).
[6]J. Moser, A. Eichler, J. Güttinger, M. Dykman, and A. Bachtold, Nat. Nanotechnol. **9**, 1007 (2014).
[7]E. Gavartin, P. Verlot, and T. Kippenberg, Nat. Nanotechnol. **7**, 509 (2012).
[8]J. Moser, J. Güttinger, A. Eichler, M. Esplandiu, D. Liu, M. Dykman, and A. Bachtold, Nat. Nanotechnol. **8**, 493 (2013).
[9]C. Reinhardt, T. Müller, A. Bourassa, and J. Sankey, Phys. Rev. X **6**, 021001 (2016).
[10]P. Saulson, Phys. Rev. D **42**, 2437 (1990).
[11]A. Ghadimi, S. Fedorov, N. Engelsen, M. Bereyhi, R. Schilling, D. Wilson, and T. Kippenberg, Science **360**, 764 (2018).
[12]Y. Tsaturyan, A. Barg, E. Polzik, and A. Schliesser, Nat. Nanotechnol. **12**, 776 (2017).
[13]A. Vinante, M. Bignotto, M. Bonaldi, M. Cerdonio, L. Conti, P. Falferi, N. Liguori, S. Longo, R. Mezzena, A. Ortolan, G. Prodi, F. Salemi, L. Taffarello, G. Vedovato, S. Vitale, and J.-P. Zendri, Phys. Rev. Lett. **101**, 033601 (2008).
[14]J. Mertz, O. Marti, and J. Mlynek, Appl. Phys. Lett. **62**, 2344 (1993).
[15]M. Aspelmeyer, T. Kippenberg, and F. Marquardt, Rev. Mod. Phys. **86**, 1391 (2014).
[16]E. Serra, M. Bawaj, A. Borrielli, G. Di Giuseppe, S. Forte, N. Kralj, N. Malossi, L. Marconi, F. Marin, F. Marino, B. Morana, R. Natali, G. Pandraud, A. Pontin, G. Prodi, M. Rossi, P. Sarro, D. Vitali, and M. Bonaldi, AIP Adv. **6**, 065004 (2016).
[17]M. Rossi, N. Kralj, S. Zippilli, R. Natali, A. Borrielli, G. Pandraud, E. Serra, G. Di Giuseppe, and D. Vitali, Phys. Rev. Lett. **119**, 123603 (2017).
[18]Y. Patil, S. Chakram, L. Chang, and M. Vengalattore, Phys. Rev. Lett. **115**, 017202 (2015).
[19]A. Chowdhury, P. Vezio, M. Bonaldi, A. Borrielli, F. Marino, B. Morana, G. Pandraud, A. Pontin, G. Prodi, P. Sarro, E. Serra, and F. Marin, Quantum Sci. Technol. **4**, 024007 (2019).
[20]P. Vezio, A. Chowdhury, M. Bonaldi, A. Borrielli, F. Marino, B. Morana, G. A. Prodi, P. M. Sarro, E. Serra, and F. Marin, Phys. Rev. A **102**, 053505 (2020).
[21]A. Chowdhury, P. Vezio, M. Bonaldi, A. Borrielli, F. Marino, B. Morana, G. Prodi, P. Sarro, E. Serra, and F. Marin, Phys. Rev. Lett. **124**, 023601 (2020).
[22]M. Poggio, C. Degen, H. Mamin, and D. Rugar, Phys. Rev. Lett. **99**, 017201 (2007).
[23]The mechanical dissipation of a resonator can be alternatively described by means of a complex spring constant $k(1 + i\phi(\omega))$, in order to take into account the phase lag $\phi(\omega)$ of the displacement behind a sinusoidal force. This damping model is more appropriate to describe resonators under low-loss intrinsic dissipation as that employed in the paper. However, as we are only interested in the spectral analysis of the motion at frequencies close to a mechanical resonance, both descriptions are equivalent. Due to the simpler physical interpretation, in the rest of the paper, we will use the velocity-damping model.[10]
[24]D. Kleckner and D. Bouwmeester, Nature **444**, 75 (2006).
[25]J. Miller, A. Ansari, D. Heinz, Y. Chen, I. Flader, D. Shin, L. Villanueva, and T. Kenny, Appl. Phys. Rev. **5**, 041307 (2018).
[26]M. Hammig and D. Wehe, IEEE Sens. J. **7**, 352 (2007).
[27]K. Lee, T. McRae, G. Harris, J. Knittel, and W. Bowen, Phys. Rev. Lett. **104**, 123604 (2010).
[28]S. I. Lee, S. W. Howell, A. Raman, and R. Reifenberger, Phys. Rev. B **66**, 115409 (2002).
[29]A. Vinante, M. Bonaldi, F. Marin, and J.-P. Zendri, Nat. Nanotechnol. **8**, 470 (2013).
[30]G. Harris, D. McAuslan, T. Stace, A. Doherty, and W. Bowen, Phys. Rev. Lett. **111**, 103603 (2013).
[31]E. Gavartin, P. Verlot, and T. Kippenberg, Nat. Commun. **4**, 2860 (2013).
[32]A. Pontin, M. Bonaldi, A. Borrielli, F. Cataliotti, F. Marino, G. Prodi, E. Serra, and F. Marin, Phys. Rev. A **89**, 023848 (2014).
[33]G. González, Classical Quantum Gravity **17**, 4409 (2000).
[34]S. Schmid, K. Jensen, K. Nielsen, and A. Boisen, Phys. Rev. B **84**, 165307 (2011).
[35]T. Purdy, P.-L. Yu, R. Peterson, N. Kampel, and C. Regal, Phys. Rev. X **3**, 031012 (2014).
[36]D. Wilson, C. Regal, S. Papp, and H. Kimble, Phys. Rev. Lett. **103**, 207204 (2009).
[37]A. Borrielli, L. Marconi, F. Marin, F. Marino, B. Morana, G. Pandraud, A. Pontin, G. Prodi, P. Sarro, E. Serra, and M. Bonaldi, Phys. Rev. B **94**, 121403 (R) (2016).
[38]E. Serra, B. Morana, A. Borrielli, F. Marin, G. Pandraud, A. Pontin, G. Prodi, P. Sarro, and M. Bonaldi, J. Microelectromech. Syst. **27**, 1193 (2018).
[39]Q. Unterreithmeier, E. Weig, and J. Kotthaus, Nature **458**, 1001 (2009).

[40]F. Buters, K. Heeck, H. Eerkens, M. Weaver, F. Luna, S. De Man, and D. Bouwmeester, Appl. Phys. Lett. **110**, 104104 (2017).
[41]S. Schmid, T. Bagci, E. Zeuthen, J. Taylor, P. Herring, M. Cassidy, C. Marcus, L. Guillermo Villanueva, B. Amato, A. Boisen, Y. Shin, J. Kong, A. Sørensen, K. Usami, and E. Polzik, J. Appl. Phys. **115**, 054513 (2014).
[42]D. Krick, P. Lenahan, and J. Kanicki, Phys. Rev. B **38**, 8226 (1988).
[43]C. Sommer and C. Genes, Phys. Rev. Lett. **123**, 203605 (2019).
[44]J. Thompson, B. Zwickl, A. Jayich, F. Marquardt, S. Girvin, and J. Harris, Nature **452**, 72 (2008).
[45]M. Poot and H. van der Zant, Phys. Rep. **511**, 273 (2012).
[46]F. Marquardt and S. Girvin, Physics **2**, 40 (2009).